IBRO Neuroscience Reports 13 (2022) 31–37

Contents lists available at ScienceDirect

IBRO Neuroscience Reports

journal homepage: www.sciencedirect.com/journal/IBRO-Neuroscience-Reports

Research Paper

Exploring the zinc-related transcriptional landscape in Alzheimer's disease

Daniel C. Shippy, Tyler K. Ulland *

Department of Pathology and Laboratory Medicine, University of Wisconsin, Madison, WI, USA

ARTICLE INFO

Keywords:
Alzheimer's disease
Zinc
Microglia
Transcriptome
Neuroinflammation

ABSTRACT

Alzheimer's disease (AD) is a progressive neurological disorder, and increasing evidence suggests AD pathology is driven by metabolic dysfunction in the brain. Zinc is the second most abundant trace element found in the human body and is required by all living organisms. Zinc is used extensively in many biological processes, and alterations in zinc levels are implicated in the pathogenesis of numerous diseases, including AD. Since small fluctuations in brain zinc levels appear to effect AD progression, we investigated the zinc-related transcriptional responses in an AD versus non-AD state using microarray and RNA-sequencing (RNA-seq) datasets from cultured cells, mice, and humans. We identified 582 zinc-related differentially expressed genes (DEG) in human dorsolateral prefrontal cortex samples of late-onset AD (LOAD) versus non-AD controls, 146 zinc-related DEG in 5XFAD versus wild-type mice, and 95 zinc-related DEG in lipopolysaccharide (LPS)-stimulated N9 microglia versus unstimulated control cells, with 19 zinc-related DEG common to all three datasets. Of the 19 common DEG, functional enrichment and network analyses identified several biological processes and molecular functions, such as mRNA destabilization and nucleic acid binding, which may be important in neuroinflammation and AD development. Furthermore, therapeutic drugs targeting zinc-related DEG in the human dataset were identified. Taken together, these data provide insights into zinc utilization for gene transcription during AD progression which may further our understanding of AD pathogenesis and could identify new targets for therapeutic strategies targeted towards AD.

1. Introduction

Alzheimer's disease (AD) is a progressive neurological disorder and is the most common form of dementia amongst older people. Although the precise mechanisms of AD pathogenesis are not completely understood, increasing evidence suggests AD pathology is driven by metabolic dysfunction in the brain (de la Monte and Tong, 2014). Recent studies have demonstrated that changes in the metabolic profiles of microglia, the primary innate immune cells of the central nervous system (CNS), are important in controlling their activation and effector functions (Keren-Shaul et al., 2017; Shippy and Ulland, 2020; Ulland et al., 2017). Furthermore, dietary regimens, such as the ketogenic diet, are being investigated as potential treatments for AD (Brownlow et al., 2013; Fortier et al., 2019; Kashiwaya et al., 2013; Shippy et al., 2020). Therefore, identifying genes involved in nutrient uptake and utilization by microglia could be valuable in further understanding AD pathogenesis.

Zinc is the second most abundant trace element found in the human body and is required by all living organisms. Zinc is used extensively in many biological processes including metabolism, immune function, and gene transcription (McClung, 2019). The human brain has the highest level of zinc compared to other organs, and zinc homeostasis is tightly regulated by zinc transporters, zinc-like regulatory proteins, and metallothioneins (Portbury and Adlard, 2017). In AD patients, elevated zinc levels are linked to increased severity of disease and amyloid-β (Aβ) levels (Religa et al., 2006). In contrast, studies suggest low concentrations of zinc may provide protection from Aβ neurotoxicity (Cardoso et al., 2005; Lovell et al., 1999). Based on these findings, both zinc chelating and zinc supplementation strategies are being investigated as AD treatments (Corona et al., 2010; Sampson et al., 2014; Wang et al., 2012).

Since zinc homeostasis is tightly regulated and small fluctuations in

Abbreviations: Aβ, amyloid-β; AD, Alzheimer's disease; BP, biological process; CC, cellular component; CNS, central nervous system; DEG, differentially expressed genes; FC, fold change; FDR, false discovery rate; GO, gene ontology; LOAD, late-onset Alzheimer's disease; LPS, lipopolysaccharide; MF, molecular function; NF-κB, nuclear factor kappa-light-chain-enhancer of activated B cells; NLRP3, nod-like receptor family pyrin domain containing 3; RIN, RNA integrity number; RNA-seq, RNA-sequencing; ZFP, zinc finger proteins.

* Corresponding author.
E-mail address: tulland@wisc.edu (T.K. Ulland).

https://doi.org/10.1016/j.ibneur.2022.06.002
Received 29 January 2022; Received in revised form 13 May 2022; Accepted 4 June 2022
Available online 7 June 2022

brain zinc levels appear to effect AD progression (Maret and Sandstead, 2006; Portbury and Adlard, 2017; Rivers-Auty et al., 2021), we investigated the zinc-related transcriptional responses in an AD versus non-AD state using microarray and RNA-sequencing (RNA-seq) datasets from cultured cells, mice, and humans. We identified 582 zinc-related differentially expressed genes (DEG) in human dorsolateral prefrontal cortex samples of late-onset AD (LOAD) versus non-AD controls, 146 zinc-related DEG in 5XFAD versus wild-type mice, and 95 zinc-related DEG in lipopolysaccharide (LPS)-stimulated N9 microglia versus unstimulated control cells, with 19 zinc-related DEG common to all three datasets. Of the 19 DEG, functional enrichment and network analyses identified several biological processes, molecular functions, and gene interactions which may be important in AD development. Additionally, therapeutic drugs targeting zinc-related DEG in the human dataset were identified suggesting new targets for therapeutic interventions directed towards AD.

2. Materials and methods

2.1. N9 RNA-seq

The N9 microglial RNA-seq dataset was published previously by our group (GSE183038) (Shippy et al., 2022). Briefly, immortalized murine N9 microglia were cultured as previously described (Righi et al., 1989). N9 microglia were seeded at a cell density of 250,000 cells/well in a 24-well tissue culture plate. Cells were stimulated with LPS (1 μg/ml) from *Escherichia coli* O111:B4 (InvivoGen) for 6 h. Three biological assays with technical replicates (n = 3) were used. RNA was extracted using a RNeasy Plus Mini Kit (Qiagen, Cat. No. 74134). Quality and quantity of RNA was assessed using an Agilent 2100 Bioanalyzer (Agilent Technologies) and a Nanodrop spectrophotometer (Thermo Scientific). All samples had an RNA integrity number (RIN) of 9.7 or higher. RNA library preparation and transcriptome sequencing were performed by Novogene using the Illumina NovaSeq 6000 Sequencing System. Bioinformatics analysis was performed by Novogene with differential expression analysis performed using the DESeq2 R package (1.20.0). Genes with false discover rate (FDR)-adjusted *P*-values < 0.05 and fold change (FC) > 1 were considered differentially expressed.

2.2. Mouse microarray

The mouse microarray has been published in a previous study (Wang et al., 2015) and the publicly available dataset (GSE65067) was used. Briefly, microglia from female 8 month old wild-type (n = 3) and 5XFAD (n = 5) mice (The Jackson Laboratory) were FACS-sorted directly into RTL-plus lysis buffer. RNA extraction from microglia was performed using an RNeasy Plus Micro Kit (Qiagen, Cat. No. 74034). Microarray hybridization (Affymetrix MoGene 1.0 ST array) and data processing were performed at the Washington University Genome Center. Raw data were normalized using the Robust Multi-Array (RMA) method and genes were pre-filtered for expression value greater than or equal to 120 expression units. This method provides a cut-off above which genes have a 95% chance of expression demonstrated in Immgen dataset, which uses the same array platform (Wang et al., 2015). *P*-values were calculated using a Student's *t*-test and FDR-adjusted *P*-values were calculated using the Benjamini and Hochberg method (Benjamini and Hochberg, 1995). Genes with FDR-adjusted *P*-values < 0.05 and FC > 1 were considered differentially expressed.

2.3. Human microarray

To better understand the role of zinc in AD pathogenesis, we examined DEG in a large human cohort studying AD using publicly available data (GSE44770) (Zhang et al., 2013). The Harvard Brain Tissue Resource Center cohort consists of 230 human dorsolateral prefrontal cortex samples which were separated by clinical diagnosis of LOAD (n = 129) and non-AD controls (n = 101). Postmortem pathological examination was used to confirm the clinical diagnosis (Zhang et al., 2013). LOAD versus non-AD control DEG were identified using GEO2R. Genes with FDR-adjusted *P*-values < 0.05 and FC > 1 were considered differentially expressed.

2.4. Gene analyses

The 19 zinc-related DEG common to all three datasets were selected for biological function analysis. The gene list was uploaded into the Database for Annotation, Visualization and Integrated Discovery (DAVID, v. 6.8) (Huang da et al., 2009a, 2009b) for Biological Process (BP), Cellular Component (CC) and Molecular Function (MF) gene ontology (GO) analyses. Each GO with a *P*-value ≤ 0.05 was considered significant. Gene-drug interactions of the zinc-related DEG in the human dataset were identified using the drug-gene interaction database (DGIdb) (Cotto et al., 2018; Freshour et al., 2021) using the default settings.

Scatterplots were created using Prism 9.0.0 (GraphPad). Venn diagrams demonstrating overlap in zinc-related DEG amongst the three datasets were generated using InteractiVenn (Heberle et al., 2015). Gene constellations identifying genes in the *Zc3h12a* regulatory network were created with ImmGen (Heng et al., 2008) using the myeloid cells reference populations option.

3. Results

3.1. AD promotes differential expression of zinc-related genes

Analysis of publicly available RNA-seq data from LPS-stimulated N9 microglia versus non-stimulated control cells revealed a total of 95 DEG with zinc-related functions (FC > 1, FDR-adjusted *P*-value < 0.05). Of these 95 DEG, 59 were up-regulated and 36 were down-regulated (Fig. 1A). Zinc finger CCCH type containing 12 A (*Zc3h12a*) was the most up-regulated zinc-related gene (FC = 11.78) and zinc finger protein 395 (*Zfp395*) was the most down-regulated zinc-related gene (FC = −4.51).

We identified 146 zinc-related DEG (FC > 1, $P < 0.05$) in publicly available transcriptional data from sorted microglia from 8-month-old 5XFAD mice, a mouse model of AD which accumulates Aβ plaques (Oakley et al., 2006), versus wild-type mice (Wang et al., 2015). Of the 146 zinc-related DEG 18 were up-regulated and 128 were down-regulated (Fig. 1B). Zinc finger, NFX1-type containing 1 (*Znfx1*) was the most upregulated zinc gene (FC = 2.43) and solute carrier family 39 (zinc transporter), member 12 (*Slc39a12*) was the most down-regulated zinc gene (FC = −2.87).

Finally, we analyzed publicly available microarray data of human dorsolateral prefrontal cortex samples from LOAD versus non-AD controls (Zhang et al., 2013). A total of 582 zinc-related DEG (FC > 1, FDR-adjusted *P*-value < 0.05) were identified with 314 up-regulated and 268 down-regulated zinc-related genes (Fig. 1C). Solute carrier family 39 (zinc transporter), member 12 (*Slc39a12*) was the most up-regulated zinc-related gene (FC = 1.28) and zinc finger, CCHC domain containing 12 (*Zcchc12*) was the most down-regulated zinc-related gene (FC = −1.31).

In total, 19 zinc-related DEG overlapped between the three datasets (Fig. 1D). A complete list of the 19 zinc-related genes and their fold change values for all three datasets is shown in Table 1. A complete list of all the zinc-related DEG found in all three datasets is shown in Supplementary Table 1.

3.2. Enrichment analysis of altered zinc-related genes

In order to further understand the potential biological relevance of the zinc-related DEG in AD, GO analyses were performed on the 19 DEG common to the three datasets. BP GO indicated the zinc-related DEG

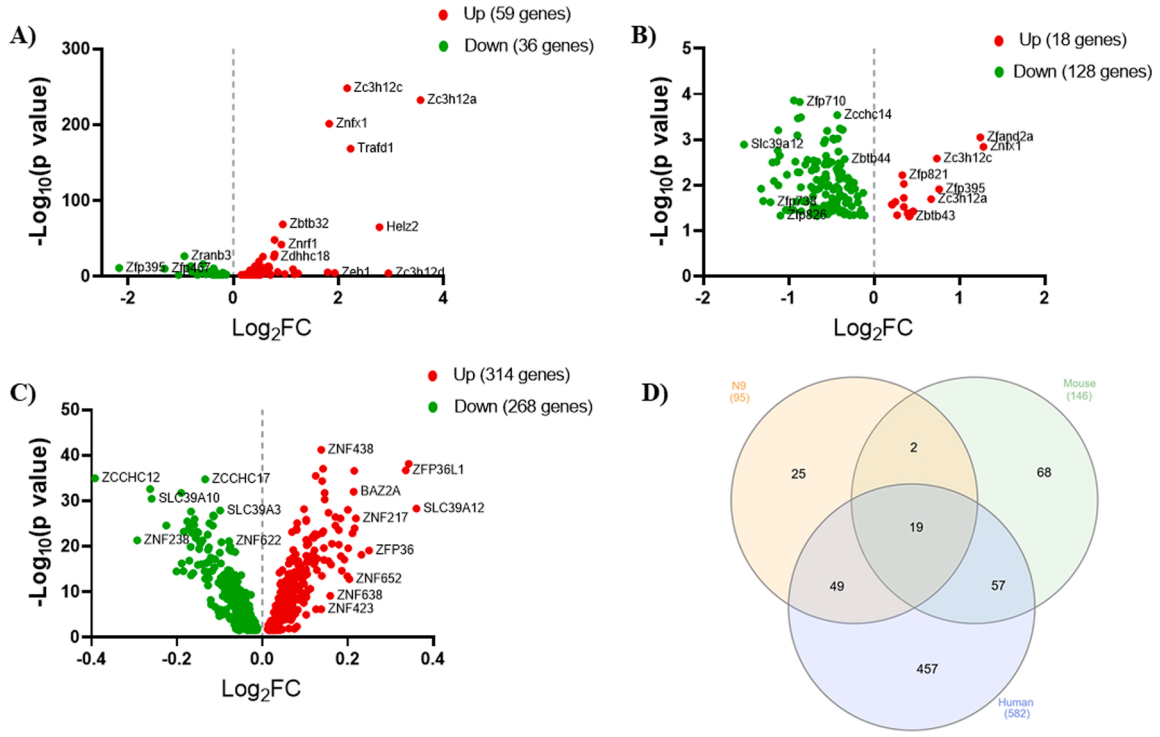

Fig. 1. Differentially expressed zinc-related genes in AD. (A) Scatter plot of zinc-related DEG (FC > 1, FDR-adjusted *P*-value < 0.05) by RNA-seq in N9 microglia stimulated with LPS (1 μg/ml) for 6 h versus unstimulated control cells. (B) Scatter plot of zinc-related DEG (FC > 1, FDR-adjusted *P*-value < 0.05) by microarray in microglia isolated from the brains of 5XFAD mice versus wild-type mice (8 months old). (C) Scatter plot of zinc-related DEG (FC > 1, FDR-adjusted *P*-value < 0.05) by microarray in human dorsolateral prefrontal cortex samples from LOAD versus non-AD controls. For all scatter plots, up-regulated genes are shown in red and down-regulated genes are shown in green. Data are graphed as $\log_2$FC versus $-\log_{10}$ (*P*-value). (D) Venn diagram demonstrating overlap in zinc-related DEG amongst the N9 cell culture, mouse microarray, and human microarray datasets.

participated in regulation of transcription, DNA-templated (*Casz1*, *Zbtb43*, *Zfp287*, *Zfp467*, *Zfp64*, *Zfp703*, *Znfx1*, *Zhx3*), transcription, DNA-templated (*Casz1*, *Zbtb43*, *Zfp287*, *Zfp467*, *Zfp64*, *Zfp703*, *Zhx3*) 3'-UTR-mediated mRNA destabilization (*Zc3h12a*, *Zfp36*), negative regulation of transcription, DNA-templated (*Zbtb38*, *Zfp703*, *Zfp706*, *Zhx3*), positive regulation of mRNA catabolic process (*Zc3h12a*, *Zfp36*), positive regulation of fat cell differentiation (*Zc3h12a*, *Zfp36*), and multicellular organism development (*Casz1*, *Zc3h12a*, *Zfp64*, *Zmym3*) (Fig. 2A). CC GO indicated the zinc-related DEG were located in the nucleus (*Casz1*, *Zc3h12a*, *Zbtb38*, *Zbtb43*, *Zfp287*, *Zfp36*, *Zfp395*, *Zfp467*, *Zfp64*, *Zfp703*, *Zfp706*, *Zfand2a*, *Zmym3*, *Znfx1*, *Zhx3*) (Fig. 2B). MF GO indicated the zinc-related DEG were involved in metal ion binding (*Casz1*, *Zc3h12a*, *Zc3h12c*, *Zbtb38*, *Zbtb43*, *Zfp287*, *Zfp36*, *Zfp395*, *Zfp467*, *Zfp608*, *Zfp64*, *Zfp644*, *Zfp703*, *Zfp706*, *Zfand2a*, *Zmym3*, *Znfx1*, *Zhx3*), DNA binding (*Casz1*, *Zc3h12a*, *Zbtb43*, *Zfp287*, *Zfp36*, *Zfp395*, *Zfp467*, *Zfp64*, *Zmym3*, *Zhx3*), nucleic acid binding (*Zbtb43*, *Zfp287*, *Zfp467*, *Zfp64*, *Zfp644*, *Zfp703*), and mRNA 3'UTR AU-rich region binding (*Zc3h12a*, *Zfp36*) (Fig. 2C).

Since *Zc3h12a* was a common zinc-related DEG in the three datasets, and involved in many of the biological processes described above, expression network analysis was performed to identify genes positively and negatively correlated with *Zc3h12a*. In the positive correlation map, several genes involved in inflammation including *Stat1* (0.744), *Eif2ak2* (0.780), and *Ifi214* (0.834) were positively correlated with *Zc3h12a* (Fig. 3A). In the negative correlation map, several genes encoding zinc finger proteins including *Zfp958* (−0.738) and *Zfp322a* (−0.770) were negatively correlated with *Zc3h12a* (Fig. 3B).

In order to determine zinc-related gene targets for therapeutic drugs, we performed gene-drug interactions in DGIdb (Cotto et al., 2018; Freshour et al., 2021) using the 582 zinc-related DEG in the human dataset. Initially, the analysis was performed on the 19 zinc-related DEG common to all three datasets, but no drugs were found to target these genes. For the human dataset, a total of 19 zinc-related DEG had interactions with therapeutic drugs (Fig. 4). Bromodomain adjacent to zinc finger domain, 2B (*Baz2b*) had the most interactions (343 drugs). Of the 343 drugs, some of the drugs are used to treat hypertension (benzthiazide, methyldopa, reserpine, nifedipine), depression (mianserin hydrochloride), and Parkinson's disease (remacemide hydrochloride). Idebenone was also identified as interacting with *Baz2b*, and this drug was originally developed for AD and other cognitive impairments, and is now under investigation as a treatment for neuromuscular diseases. A complete list of the zinc-related DEG and their associated drugs is shown in Supplementary Table 2.

4. Discussion

Using cell culture, mouse, and human gene expression datasets, we identified 19 common zinc-related DEG which may be important in AD disease processes. Several previous studies report lower zinc serum levels in AD patients (Li et al., 2017; Ventriglia et al., 2015). Other evidence suggests excessive zinc supplementation could lead to AD progression by enhancing amyloid (Flinn et al., 2014) and tau (Craven et al., 2018) pathology. Based on this evidence, it appears zinc accumulation in the brain is a tightly controlled process, with small fluctuations in zinc concentrations having large effects on disease status and other biological processes (Maret and Sandstead, 2006; Portbury and Adlard, 2017; Rivers-Auty et al., 2021). Therefore, the identification of genes involved in zinc transport and utilization could be important in further understanding AD pathogenesis.

Neuroinflammation plays a major role in AD pathogenesis by exacerbating both amyloid and tau pathologies (Heppner et al., 2015). Zinc homeostasis is crucial for maintaining a healthy immune system, and zinc deficiency often elevates the inflammatory response (Gammoh and Rink, 2017). Activation of nuclear factor kappa-light-chain-enhancer of

Table 1
Altered zinc-related genes common to N9 cell culture, mouse microarray, and human microarray datasets.

Gene[a]	Gene Description	N9 Cell Culture FC	Mouse Microarray FC	Human Microarray FC
Casz1	castor zinc finger 1	2.34	1.27	1.05
Zbtb38	zinc finger and BTB domain containing 38	1.22	-1.40	1.03
Zbtb43	zinc finger and BTB domain containing 43	1.28	1.33	1.02
Zc3h12a	zinc finger CCCH type containing 12A	11.78	1.59	1.07
Zc3h12c	zinc finger CCCH type containing 12C	4.48	1.66	1.11
Zdhhc14	zinc finger, DHHC domain containing 14	-1.79	-1.81	-1.02
Zfand2a	zinc finger, AN1-type domain 2A	1.11	2.37	-1.05
Zfp36	zinc finger protein 36	1.44	-1.23	1.19
Zfp64	zinc finger protein 64	1.16	-1.12	-1.09
Zfp287	zinc finger protein 287	1.36	-1.33	-1.03
Zfp395	zinc finger protein 395	-4.51	1.69	1.13
Zfp467	zinc finger protein 467	-2.47	-1.32	1.02
Zfp608	zinc finger protein 608	-1.73	-1.39	1.05
Zfp644	zinc finger protein 644	1.23	-1.30	1.05
Zfp703	zinc finger protein 703	1.39	1.34	1.05
Zfp706	zinc finger protein 706	-1.10	-1.32	-1.11
Zhx3	zinc fingers and homeoboxes 3	-1.42	-1.41	1.09
Zmym3	zinc finger, MYM-type 3	-1.44	-1.53	1.02
Znfx1	zinc finger, NFX1-type containing 1	3.53	2.43	1.06

[a] Mouse gene name.

activated B cells (NF-κB) and the nod-like receptor family pyrin domain containing 3 (NLRP3) inflammasome are important mechanisms in chronic neuroinflammation that significantly increase AD pathology (Granic et al., 2009; Heneka et al., 2013). Zinc deficiency has been shown to exacerbate cognitive decline by enhancement of the NLRP3 inflammasome in a mouse model of AD (Bales et al., 1998; Rivers-Auty et al., 2021). In our study, gene correlation analysis of one of the most altered zinc genes, *Zc3h12a*, shows strong relationships with several inflammatory genes including *Ifi207*, *Ifi213*, and *Ifi214*, as well as *Stat1*, a transcriptional activator of the inflammatory response. Therefore, it is important to identify zinc-related DEG in the context of AD as the role of zinc homeostasis in AD-driven neuroinflammation is further investigated.

Zinc finger proteins (ZFP) are amongst the most abundant proteins in the eukaryotic genome with a wide array of functions including lipid binding, regulation of apoptosis, DNA recognition, transcriptional activation, RNA packaging, and protein folding and assembly (Laity et al., 2001). In our study, nine genes encoding ZFP were differentially expressed in all three datasets. The *Zfp36* gene encodes the RNA-binding protein tristetraprolin, which induces mRNA degradation of key genes in the inflammatory response (Molle et al., 2013). Moreover, a recent study suggests tristetraprolin degrades NLRP3 mRNA leading to a significant decrease in inflammasome activation (Bertesi et al., 2020). Recently, gene therapy with ZFP transcription factors has emerged as a potential treatment for tau-related human brain diseases (Wegmann et al., 2021). In this study, tau mRNA was significantly reduced, leading to rescued neuronal damage around Aβ plaques in a mouse model of AD (Wegmann et al., 2021). Taken together, these studies support the continued investigation of zinc for potential therapies of AD.

AD drug development has been especially arduous, with approximately 99% of trials showing no difference between the treated and placebo groups (Cummings et al., 2017, 2014). To date, many of the therapeutic agents developed for AD have focused on amyloid and tau reduction (Congdon and Sigurdsson, 2018; Pinheiro and Faustino, 2019). In our study, gene-drug analysis of the altered zinc-related genes in the human dataset identified drugs targeting zinc-related DEG in our study. The *Baz2b* gene had the most interactions (343 drugs) with several drugs used to treat hypertension. Hypertension is one of the most prevalent medical conditions with over 1.3 billion people diagnosed worldwide (Bloch, 2016). Several animal studies show a direct relationship with hypertension and neuroinflammation and amyloid deposition (Carnevale et al., 2012; Kruyer et al., 2015) while postmortem studies in humans have shown mid-life hypertension increased amyloid and neurofibrillary tangles (Petrovitch et al., 2000; Shah et al., 2012). Idebenone was also identified as a target of *Baz2b* in our study. Idebenone was initially developed as an AD drug (Weyer et al., 1997), but is now being investigated for the neuromuscular diseases Friedreich's ataxia and Duchenne muscular dystrophy (Artuch et al., 2002; Buyse et al., 2015). Overall, there is a clear need for the development of new drugs for AD, and these data could assist in the identification of new targets for therapeutic strategies directed towards AD.

As with most gene expression analyses, there are strengths and weaknesses associated with our study identifying zinc-related DEG in AD. A major advantage of our study is that common zinc-related DEG were identified from three distinct AD datasets (cell culture, mouse, and human) which strengthens the probability of zinc being involved in AD progression. In contrast, most of the zinc-related DEG, especially in the human dataset, were not greatly altered. Furthermore, there was not a strong consensus amongst the 19 zinc-related DEG common to the three datasets, as only eight of the 19 showed the same directional change in expression. This could possibly be due to the tightly controlled regulation of zinc in the human brain, making it plausible that small alterations in the zinc-related genes could lead to large biological effects. Also, although not in the N9 cell culture dataset, and thus not in the list of common zinc-related DEG, *Slc39a12* was the most down-regulated gene in the mouse dataset, while being the most up-regulated gene in the human dataset. Differences in collection methods between the two studies could be a possible explanation for the contrasting results, as the mouse dataset is from RNA isolated from microglia, and the human dataset is from RNA isolated from dorsolateral prefrontal cortex samples. A previous study, however, indicates humans have higher densities of microglia in the dorsolateral prefrontal cortex during AD (Edler et al., 2018), and the alteration of *Slc39a12* in the human dataset used in our study is similar to a study using single-cell RNA-seq from a microglia cluster in human dorsolateral prefrontal cortex samples (Zhou et al., 2020). Overall, studies comparing the transcriptional signature of microglia in AD in mice and humans have been mixed, with some indicating that the response may be similar (Sobue et al., 2021; Ulland et al., 2017) and some studies indicating that the response may be different (Olah et al., 2020; Zhou et al., 2020). These results are anticipated, as human disease consists of both neurofibrillary tangles and Aβ plaques compared to the 5XFAD mouse model in which only plaques form. Therefore, it is important to consider all models of AD when identifying gene network mechanisms in AD progression.

5. Conclusions

Overall, we used publicly available datasets to identify 582 zinc-related DEG in human dorsolateral prefrontal cortex samples of LOAD versus non-AD controls, 146 zinc-related DEG in 5XFAD versus wild-type mice, and 95 zinc-related DEG in LPS-stimulated N9 microglia

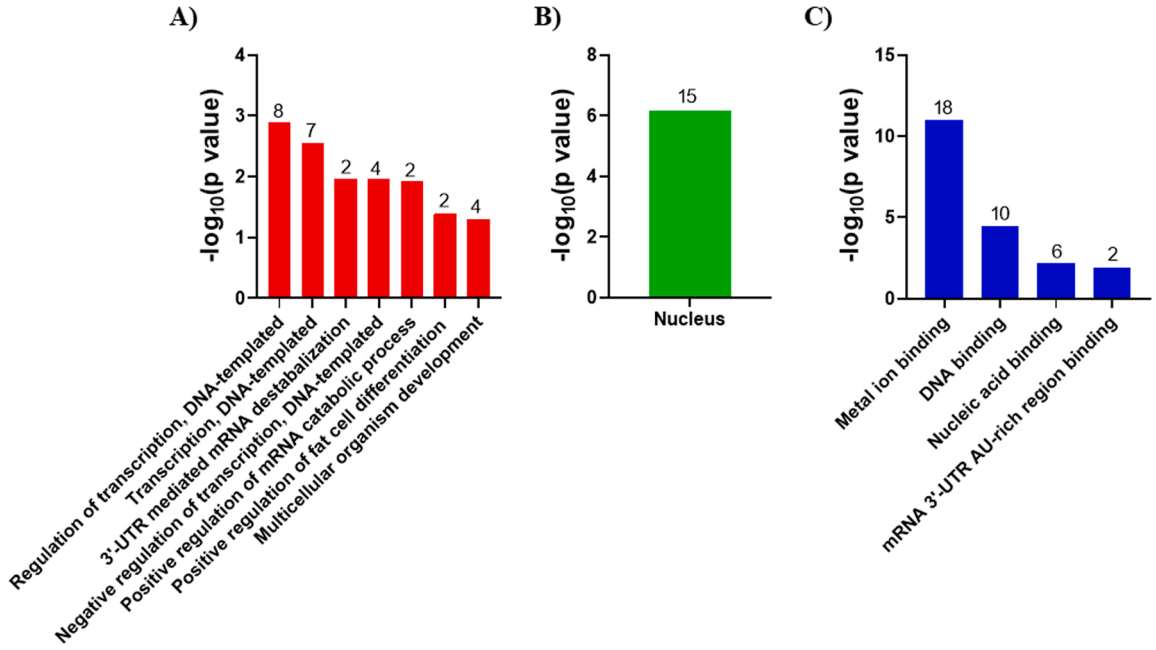

Fig. 2. GO enrichment analysis. Biological function analyses for the 19 zinc-related DEG common to the three datasets was performed using DAVID. Analyses were performed for Biological Process (BP) (A), Cellular Component (CC) (B), and Molecular Function (MF) (C). Pathways are shown in descending order based on $-\log_{10}$ *P*-values. The number of genes associated with each GO term is shown above each bar. Only GO terms with a *P*-value ≤ 0.05 are shown.

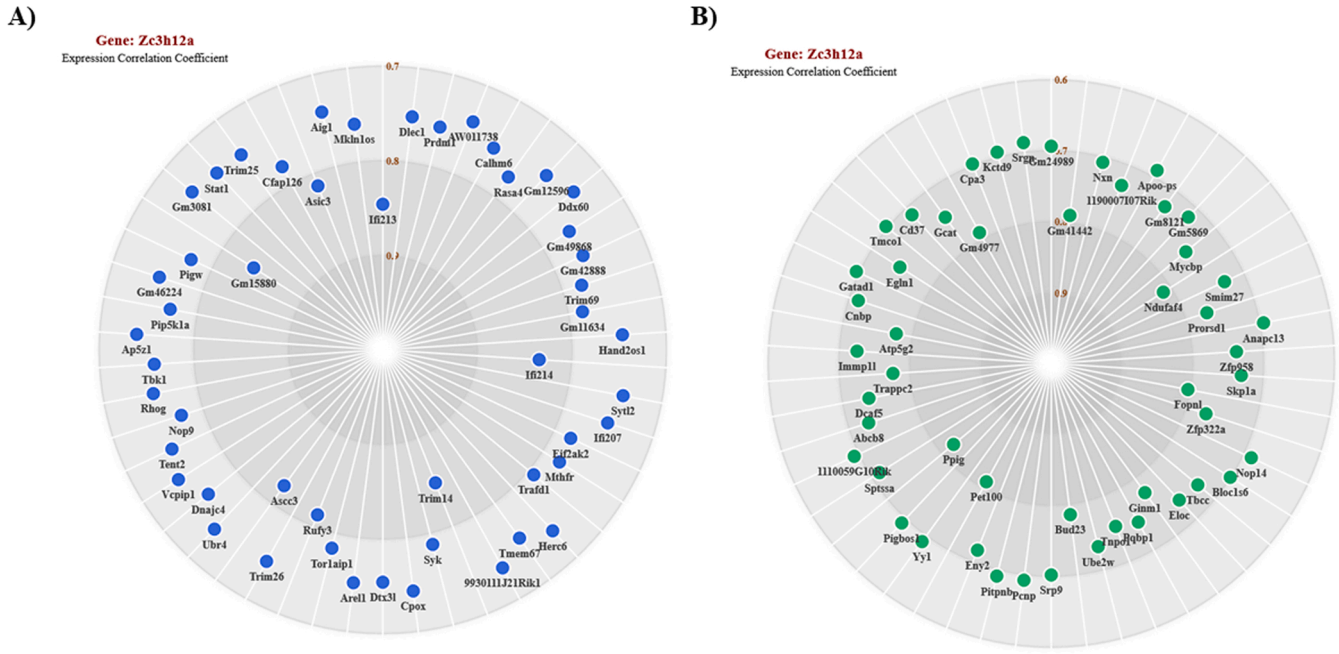

Fig. 3. *Zc3h12a* expression network analysis. Gene constellations for *Zc3h12a* were created using ImmGen. (A) Positive expression correlation of genes to *Zc3h12a*. (B) Negative expression correlation of genes to *Zc3h12a*. The numbers in parentheses are the expression correlation coefficients.

versus unstimulated control cells, with 19 zinc-related DEG common to all three datasets. Of the 19 zinc-related DEG, functional enrichment and network analyses identified several biological processes, molecular functions, and gene interactions which may be important in AD development. Furthermore, therapeutic drugs targeting zinc-related DEG in the human dataset were identified. Taken together, these data provide insights into zinc utilization during AD progression which may further our understanding of AD pathogenesis and could identify new targets for therapeutic strategies for AD.

Funding

This work was supported by the National Institutes of Health R21AG068652.

CRediT author contribution statement

Daniel C. Shippy: Conceptualization, Investigation, Data curation, Formal analysis, Methodology, Writing – original draft. **Tyler K.**

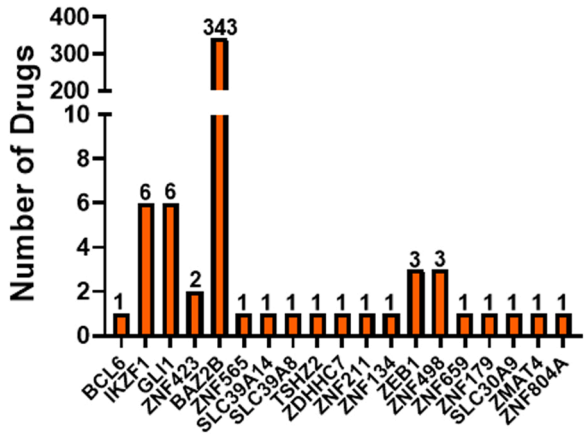

Fig. 4. Gene-drug interactions. Interactions between therapeutic drugs and the zinc-related DEG in the human dataset. Genes identified with drug interactions are shown and the number of drugs associated with each gene is shown above each bar.

Ulland: Conceptualization, Supervision, Funding acquisition, Writing – review & editing.

Conflicts of interest

None.

Data Availability

The datasets generated and/or analyzed during the current study are available in the Gene Expression Omnibus (GEO) repository, GSE65067, GSE183038, and GSE44770.

Acknowledgements

We thank Jyoti Watters for assistance in acquiring the N9 microglial cell line. We thank Paula Ricciardi-Castagnoli for the N9 microglial cells.

Appendix A. Supporting information

Supplementary data associated with this article can be found in the online version at doi:10.1016/j.ibneur.2022.06.002.

References

Artuch, R., Aracil, A., Mas, A., Colome, C., Rissech, M., Monros, E., Pineda, M., 2002. Friedreich's ataxia: idebenone treatment in early stage patients. Neuropediatrics 33, 190–193.
Bales, K.R., Du, Y., Dodel, R.C., Yan, G.M., Hamilton-Byrd, E., Paul, S.M., 1998. The NF-kappaB/Rel family of proteins mediates Abeta-induced neurotoxicity and glial activation. Brain Res. Mol. Brain Res. 57, 63–72.
Benjamini, Y., Hochberg, Y., 1995. Controlling the false discovery rate - a practical and powerful approach to multiple testing. J. R. Stat. Soc. B 57, 289–300.
Bertesi, M., Fantini, S., Alecci, C., Lotti, R., Martello, A., Parenti, S., Carretta, C., Marconi, A., Grande, A., Pincelli, C., Zanocco-Marani, T., 2020. Promoter methylation leads to decreased ZFP36 expression and deregulated NLRP3 inflammasome activation in psoriatic fibroblasts. Front. Med. 7, 579383.
Bloch, M.J., 2016. Worldwide prevalence of hypertension exceeds 1.3 billion. J. Am. Soc. Hypertens. 10, 753–754.
Brownlow, M.L., Benner, L., D'Agostino, D., Gordon, M.N., Morgan, D., 2013. Ketogenic diet improves motor performance but not cognition in two mouse models of Alzheimer's pathology. PLoS One 8, e75713.
Buyse, G.M., Voit, T., Schara, U., Straathof, C.S.M., D'Angelo, M.G., Bernert, G., Cuisset, J.M., Finkel, R.S., Goemans, N., McDonald, C.M., Rummey, C., Meier, T., Group, D.S., 2015. Efficacy of idebenone on respiratory function in patients with Duchenne muscular dystrophy not using glucocorticoids (DELOS): a double-blind randomised placebo-controlled phase 3 trial. Lancet 385, 1748–1757.
Cardoso, S.M., Rego, A.C., Pereira, C., Oliveira, C.R., 2005. Protective effect of zinc on amyloid-beta 25-35 and 1-40 mediated toxicity. Neurotox. Res. 7, 273–281.
Carnevale, D., Mascio, G., Ajmone-Cat, M.A., D'Andrea, I., Cifelli, G., Madonna, M., Cocozza, G., Frati, A., Carullo, P., Carnevale, L., Alleva, E., Branchi, I., Lembo, G., Minghetti, L., 2012. Role of neuroinflammation in hypertension-induced brain amyloid pathology. Neurobiol. Aging 33 (205), e219–229.
Congdon, E.E., Sigurdsson, E.M., 2018. Tau-targeting therapies for Alzheimer disease. Nat. Rev. Neurol. 14, 399–415.
Corona, C., Masciopinto, F., Silvestri, E., Viscovo, A.D., Lattanzio, R., Sorda, R.L., Ciavardelli, D., Goglia, F., Piantelli, M., Canzoniero, L.M., Sensi, S.L., 2010. Dietary zinc supplementation of 3xTg-AD mice increases BDNF levels and prevents cognitive deficits as well as mitochondrial dysfunction. Cell Death Dis. 1, e91.
Cotto, K.C., Wagner, A.H., Feng, Y.Y., Kiwala, S., Coffman, A.C., Spies, G., Wollam, A., Spies, N.C., Griffith, O.L., Griffith, M., 2018. DGIdb 3.0: a redesign and expansion of the drug-gene interaction database. Nucleic Acids Res. 46, D1068–D1073.
Craven, K.M., Kochen, W.R., Hernandez, C.M., Flinn, J.M., 2018. Zinc exacerbates tau pathology in a Tau Mouse Model. J. Alzheimers Dis. 64, 617–630.
Cummings, J., Lee, G., Mortsdorf, T., Ritter, A., Zhong, K., 2017. Alzheimer's disease drug development pipeline: 2017. Alzheimers Dement 3, 367–384.
Cummings, J.L., Morstorf, T., Zhong, K., 2014. Alzheimer's disease drug-development pipeline: few candidates, frequent failures. Alzheimers Res. Ther. 6, 37.
de la Monte, S.M., Tong, M., 2014. Brain metabolic dysfunction at the core of Alzheimer's disease. Biochem. Pharmacol. 88, 548–559.
Edler, M.K., Sherwood, C.C., Meindl, R.S., Munger, E.L., Hopkins, W.D., Ely, J.J., Erwin, J.M., Perl, D.P., Mufson, E.J., Hof, P.R., Raghanti, M.A., 2018. Microglia changes associated to Alzheimer's disease pathology in aged chimpanzees. J. Comp. Neurol. 526, 2921–2936.
Flinn, J.M., Bozzelli, P.L., Adlard, P.A., Railey, A.M., 2014. Spatial memory deficits in a mouse model of late-onset Alzheimer's disease are caused by zinc supplementation and correlate with amyloid-beta levels. Front. Aging Neurosci. 6, 174.
Fortier, M., Castellano, C.A., Croteau, E., Langlois, F., Bocti, C., St-Pierre, V., Vandenberghe, C., Bernier, M., Roy, M., Descoteaux, M., Whittingstall, K., Lepage, M., Turcotte, E.E., Fulop, T., Cunnane, S.C., 2019. A ketogenic drink improves brain energy and some measures of cognition in mild cognitive impairment. Alzheimers Dement 15, 625–634.
Freshour, S.L., Kiwala, S., Cotto, K.C., Coffman, A.C., McMichael, J.F., Song, J.J., Griffith, M., Griffith, O.L., Wagner, A.H., 2021. Integration of the Drug-Gene Interaction Database (DGIdb 4.0) with open crowdsource efforts. Nucleic Acids Res. 49, D1144–D1151.
Gammoh, N.Z., Rink, L., 2017. Zinc in Infection and Inflammation. Nutrients 9.
Granic, I., Dolga, A.M., Nijholt, I.M., van Dijk, G., Eisel, U.L., 2009. Inflammation and NF-kappaB in Alzheimer's disease and diabetes. J. Alzheimers Dis. 16, 809–821.
Heberle, H., Meirelles, G.V., da Silva, F.R., Telles, G.P., Minghim, R., 2015. InteractiVenn: a web-based tool for the analysis of sets through Venn diagrams. BMC Bioinform. 16, 169.
Heneka, M.T., Kummer, M.P., Stutz, A., Delekate, A., Schwartz, S., Vieira-Saecker, A., Griep, A., Axt, D., Remus, A., Tzeng, T.C., Gelpi, E., Halle, A., Korte, M., Latz, E., Golenbock, D.T., 2013. NLRP3 is activated in Alzheimer's disease and contributes to pathology in APP/PS1 mice. Nature 493, 674–678.
Heng, T.S., Painter, M.W., Immunological Genome Project, C., 2008. The Immunological Genome Project: networks of gene expression in immune cells. Nat. Immunol. 9, 1091–1094.
Heppner, F.L., Ransohoff, R.M., Becher, B., 2015. Immune attack: the role of inflammation in Alzheimer disease. Nat. Rev. Neurosci. 16, 358–372.
Huang da, W., Sherman, B.T., Lempicki, R.A., 2009a. Bioinformatics enrichment tools: paths toward the comprehensive functional analysis of large gene lists. Nucleic Acids Res. 37, 1–13.
Huang da, W., Sherman, B.T., Lempicki, R.A., 2009b. Systematic and integrative analysis of large gene lists using DAVID bioinformatics resources. Nat. Protoc. 4, 44–57.
Kashiwaya, Y., Bergman, C., Lee, J.H., Wan, R., King, M.T., Mughal, M.R., Okun, E., Clarke, K., Mattson, M.P., Veech, R.L., 2013. A ketone ester diet exhibits anxiolytic and cognition-sparing properties, and lessens amyloid and tau pathologies in a mouse model of Alzheimer's disease. Neurobiol. Aging 34, 1530–1539.
Keren-Shaul, H., Spinrad, A., Weiner, A., Matcovitch-Natan, O., Dvir-Szternfeld, R., Ulland, T.K., David, E., Baruch, K., Lara-Astaiso, D., Toth, B., Itzkovitz, S., Colonna, M., Schwartz, M., Amit, I., 2017. A unique microglia type associated with restricting development of Alzheimer's disease. Cell 169, 1276–1290 e1217.
Kruyer, A., Soplop, N., Strickland, S., Norris, E.H., 2015. Chronic hypertension leads to neurodegeneration in the TgSwDI mouse model of Alzheimer's disease. Hypertension 66, 175–182.
Laity, J.H., Lee, B.M., Wright, P.E., 2001. Zinc finger proteins: new insights into structural and functional diversity. Curr. Opin. Struct. Biol. 11, 39–46.
Li, D.D., Zhang, W., Wang, Z.Y., Zhao, P., 2017. Serum copper, zinc, and iron levels in patients with Alzheimer's disease: a meta-analysis of case-control studies. Front. Aging Neurosci. 9, 300.
Lovell, M.A., Xie, C., Markesbery, W.R., 1999. Protection against amyloid beta peptide toxicity by zinc. Brain Res. 823, 88–95.
Maret, W., Sandstead, H.H., 2006. Zinc requirements and the risks and benefits of zinc supplementation. J. Trace Elem. Med. Biol. 20, 3–18.
McClung, J.P., 2019. Iron, zinc, and physical performance. Biol. Trace Elem. Res. 188, 135–139.
Molle, C., Zhang, T., Ysebrant de Lendonck, L., Gueydan, C., Andrianne, M., Sherer, F., Van Simaeys, G., Blackshear, P.J., Leo, O., Goriely, S., 2013. Tristetraprolin regulation of interleukin 23 mRNA stability prevents a spontaneous inflammatory disease. J. Exp. Med. 210, 1675–1684.
Oakley, H., Cole, S.L., Logan, S., Maus, E., Shao, P., Craft, J., Guillozet-Bongaarts, A., Ohno, M., Disterhoft, J., Van Eldik, L., Berry, R., Vassar, R., 2006. Intraneuronal beta-amyloid aggregates, neurodegeneration, and neuron loss in transgenic mice with five familial Alzheimer's disease mutations: potential factors in amyloid plaque formation. J. Neurosci. 26, 10129–10140.

Olah, M., Menon, V., Habib, N., Taga, M.F., Ma, Y., Yung, C.J., Cimpean, M., Khairallah, A., Coronas-Samano, G., Sankowski, R., Grun, D., Kroshilina, A.A., Dionne, D., Sarkis, R.A., Cosgrove, G.R., Helgager, J., Golden, J.A., Pennell, P.B., Prinz, M., Vonsattel, J.P.G., Teich, A.F., Schneider, J.A., Bennett, D.A., Regev, A., Elyaman, W., Bradshaw, E.M., De Jager, P.L., 2020. Single cell RNA sequencing of human microglia uncovers a subset associated with Alzheimer's disease. Nat. Commun. 11, 6129.

Petrovitch, H., White, L.R., Izmirilian, G., Ross, G.W., Havlik, R.J., Markesbery, W., Nelson, J., Davis, D.G., Hardman, J., Foley, D.J., Launer, L.J., 2000. Midlife blood pressure and neuritic plaques, neurofibrillary tangles, and brain weight at death: the HAAS. Honolulu-Asia aging Study. Neurobiol. Aging 21, 57–62.

Pinheiro, L., Faustino, C., 2019. Therapeutic strategies targeting amyloid-beta in Alzheimer's Disease. Curr. Alzheimer Res. 16, 418–452.

Portbury, S.D., Adlard, P.A., 2017. Zinc signal in brain diseases. Int. J. Mol. Sci. 18.

Religa, D., Strozyk, D., Cherny, R.A., Volitakis, I., Haroutunian, V., Winblad, B., Naslund, J., Bush, A.I., 2006. Elevated cortical zinc in Alzheimer disease. Neurology 67, 69–75.

Righi, M., Mori, L., De Libero, G., Sironi, M., Biondi, A., Mantovani, A., Donini, S.D., Ricciardi-Castagnoli, P., 1989. Monokine production by microglial cell clones. Eur. J. Immunol. 19, 1443–1448.

Rivers-Auty, J., Tapia, V.S., White, C.S., Daniels, M.J.D., Drinkall, S., Kennedy, P.T., Spence, H.G., Yu, S., Green, J.P., Hoyle, C., Cook, J., Bradley, A., Mather, A.E., Peters, R., Tzeng, T.C., Gordon, M.J., Beattie, J.H., Brough, D., Lawrence, C.B., 2021. Zinc status alters Alzheimer's disease progression through NLRP3-Dependent inflammation. J. Neurosci. 41, 3025–3038.

Sampson, E.L., Jenagaratnam, L., McShane, R., 2014. Metal protein attenuating compounds for the treatment of Alzheimer's dementia. Cochrane Database Syst. Rev. CD005380.

Shah, N.S., Vidal, J.S., Masaki, K., Petrovitch, H., Ross, G.W., Tilley, C., DeMattos, R.B., Tracy, R.P., White, L.R., Launer, L.J., 2012. Midlife blood pressure, plasma beta-amyloid, and the risk for Alzheimer disease: the Honolulu Asia Aging Study. Hypertension 59, 780–786.

Shippy, D.C., Ulland, T.K., 2020. Microglial immunometabolism in Alzheimer's disease. Front. Cell Neurosci. 14, 563446.

Shippy, D.C., Watters, J.J., Ulland, T.K., 2022. Transcriptional response of murine microglia in Alzheimer's disease and inflammation. BMC Genom. 23, 183.

Shippy, D.C., Wilhelm, C., Viharkumar, P.A., Raife, T.J., Ulland, T.K., 2020. beta-Hydroxybutyrate inhibits inflammasome activation to attenuate Alzheimer's disease pathology. J. Neuroinflamm. 17, 280.

Sobue, A., Komine, O., Hara, Y., Endo, F., Mizoguchi, H., Watanabe, S., Murayama, S., Saito, T., Saido, T.C., Sahara, N., Higuchi, M., Ogi, T., Yamanaka, K., 2021. Microglial gene signature reveals loss of homeostatic microglia associated with neurodegeneration of Alzheimer's disease. Acta Neuropathol. Commun. 9, 1.

Ulland, T.K., Song, W.M., Huang, S.C., Ulrich, J.D., Sergushichev, A., Beatty, W.L., Loboda, A.A., Zhou, Y., Cairns, N.J., Kambal, A., Loginicheva, E., Gilfillan, S., Cella, M., Virgin, H.W., Unanue, E.R., Huang, Y., Artyomov, M.N., Holtzman, D.M., Colonna, M., 2017. TREM2 maintains microglial metabolic fitness in Alzheimer's disease. Cell 170, 649–663 e613.

Ventriglia, M., Brewer, G.J., Simonelli, I., Mariani, S., Siotto, M., Bucossi, S., Squitti, R., 2015. Zinc in Alzheimer's disease: a meta-analysis of serum, plasma, and cerebrospinal fluid studies. J. Alzheimers Dis. 46, 75–87.

Wang, T., Wang, C.Y., Shan, Z.Y., Teng, W.P., Wang, Z.Y., 2012. Clioquinol reduces zinc accumulation in neuritic plaques and inhibits the amyloidogenic pathway in AbetaPP/PS1 transgenic mouse brain. J. Alzheimers Dis. 29, 549–559.

Wang, Y., Cella, M., Mallinson, K., Ulrich, J.D., Young, K.L., Robinette, M.L., Gilfillan, S., Krishnan, G.M., Sudhakar, S., Zinselmeyer, B.H., Holtzman, D.M., Cirrito, J.R., Colonna, M., 2015. TREM2 lipid sensing sustains the microglial response in an Alzheimer's disease model. Cell 160, 1061–1071.

Wegmann, S., DeVos, S.L., Zeitler, B., Marlen, K., Bennett, R.E., Perez-Rando, M., MacKenzie, D., Yu, Q., Commins, C., Bannon, R.N., Corjuc, B.T., Chase, A., Diez, L., Nguyen, H.B., Hinkley, S., Zhang, L., Goodwin, A., Ledeboer, A., Lam, S., Ankoudinova, I., Tran, H., Scarlott, N., Amora, R., Surosky, R., Miller, J.C., Robbins, A.B., Rebar, E.J., Urnov, F.D., Holmes, M.C., Pooler, A.M., Riley, B., Zhang, H.S., Hyman, B.T., 2021. Persistent repression of tau in the brain using engineered zinc finger protein transcription factors. Sci. Adv. 7.

Weyer, G., Babej-Dolle, R.M., Hadler, D., Hofmann, S., Herrmann, W.M., 1997. A controlled study of 2 doses of idebenone in the treatment of Alzheimer's disease. Neuropsychobiology 36, 73–82.

Zhang, B., Gaiteri, C., Bodea, L.G., Wang, Z., McElwee, J., Podtelezhnikov, A.A., Zhang, C., Xie, T., Tran, L., Dobrin, R., Fluder, E., Clurman, B., Melquist, S., Narayanan, M., Suver, C., Shah, H., Mahajan, M., Gillis, T., Mysore, J., MacDonald, M.E., Lamb, J.R., Bennett, D.A., Molony, C., Stone, D.J., Gudnason, V., Myers, A.J., Schadt, E.E., Neumann, H., Zhu, J., Emilsson, V., 2013. Integrated systems approach identifies genetic nodes and networks in late-onset Alzheimer's disease. Cell 153, 707–720.

Zhou, Y., Song, W.M., Andhey, P.S., Swain, A., Levy, T., Miller, K.R., Poliani, P.L., Cominelli, M., Grover, S., Gilfillan, S., Cella, M., Ulland, T.K., Zaitsev, K., Miyashita, A., Ikeuchi, T., Sainouchi, M., Kakita, A., Bennett, D.A., Schneider, J.A., Nichols, M.R., Beausoleil, S.A., Ulrich, J.D., Holtzman, D.M., Artyomov, M.N., Colonna, M., 2020. Human and mouse single-nucleus transcriptomics reveal TREM2-dependent and TREM2-independent cellular responses in Alzheimer's disease. Nat. Med. 26, 131–142.